Regular Article

Tissue-specific Physical and Biological Microenvironments Modulate the Behavior of Cervical Squamous Cell Carcinoma

Katsuyuki Hanashima[1,2], Takashi Akutagawa[1], Mihoko Yamamoto-Rikitake[1], Takehisa Sakumoto[1], Maki Futamata[1], Yoshifumi Nakao[2], Masatoshi Yokoyama[2], Shuji Toda[1,3] and Shigehisa Aoki[1]

[1]Department of Pathology and Microbiology, Faculty of Medicine, Saga University, 5–1–1 Nabeshima, Saga, Saga 849–8501, Japan, [2]Department of Obstetrics and Gynecology, Faculty of Medicine, Saga University, 5–1–1 Nabeshima, Saga, Saga 849–8501, Japan and [3]Department of Pathology, Takagi Hospital, Okawa, Fukuoka 831–8501, Japan

The mechanisms controlling the aggressiveness and survival of cervical SCC cells remain unclear. We investigated how the physical and biological microenvironments regulate the growth, apoptosis and invasiveness of cervical cancer cells. Dynamic flow and air exposure were evaluated as physical microenvironmental factors, and stromal fibroblasts were evaluated as a biological microenvironmental factor. To investigate any regulatory effects of these microenvironmental factors, we established a new culture model which concurrently replicates fluid streaming, air exposure and cancer-stromal interactions. Three cervical cancer cell lines were cultured with or without NIH 3T3 fibroblasts. Air exposure was realized using a double-dish culture system. Dynamic flow was created using a rotary shaker. Dynamic flow and air exposure promoted the proliferative activity and decreased the apoptosis of cervical cancer cells. Fibroblasts regulated the invasive ability, growth and apoptosis of cervical cancer cells. Extracellular signal-regulated kinase and p38 signaling were regulated either synergistically or independently by dynamic flow, air exposure and cellular interactions, depending on the cervical cancer cell type. This study demonstrates that the physical and biological microenvironments interact to regulate the aggressiveness and survival of cervical cancer cells. Our simple culture system is a promising model for developing further treatment strategies for various types of cancer.

Key words: cervical cancer, cancer microenvironment, cancer-stroma interaction, shear stress, air-liquid interface

I. Introduction

Cervical cancer is the most common gynecological malignancy and accounts for around 570,000 new cases and about 311,000 deaths per year worldwide [3]. Most cases of cervical cancer are caused by persistent infection with one of about 15 genotypes of carcinogenic human papillomavirus (HPV) [25]. Although considerable advances have been made in our understanding of the carcinogenesis of cervical cancer, the factors that control the aggressiveness of cervical cancer cells have not been unequivocally elucidated.

Recently, the cancer microenvironment has received widespread attention as a factor regulating cancer cell kinetics [9, 21]. The microenvironment of a tumor consists of biological and physical factors that regulate the homeostasis and invasiveness of cancer cells. For example, cell-cell interactions and physical stimulation from
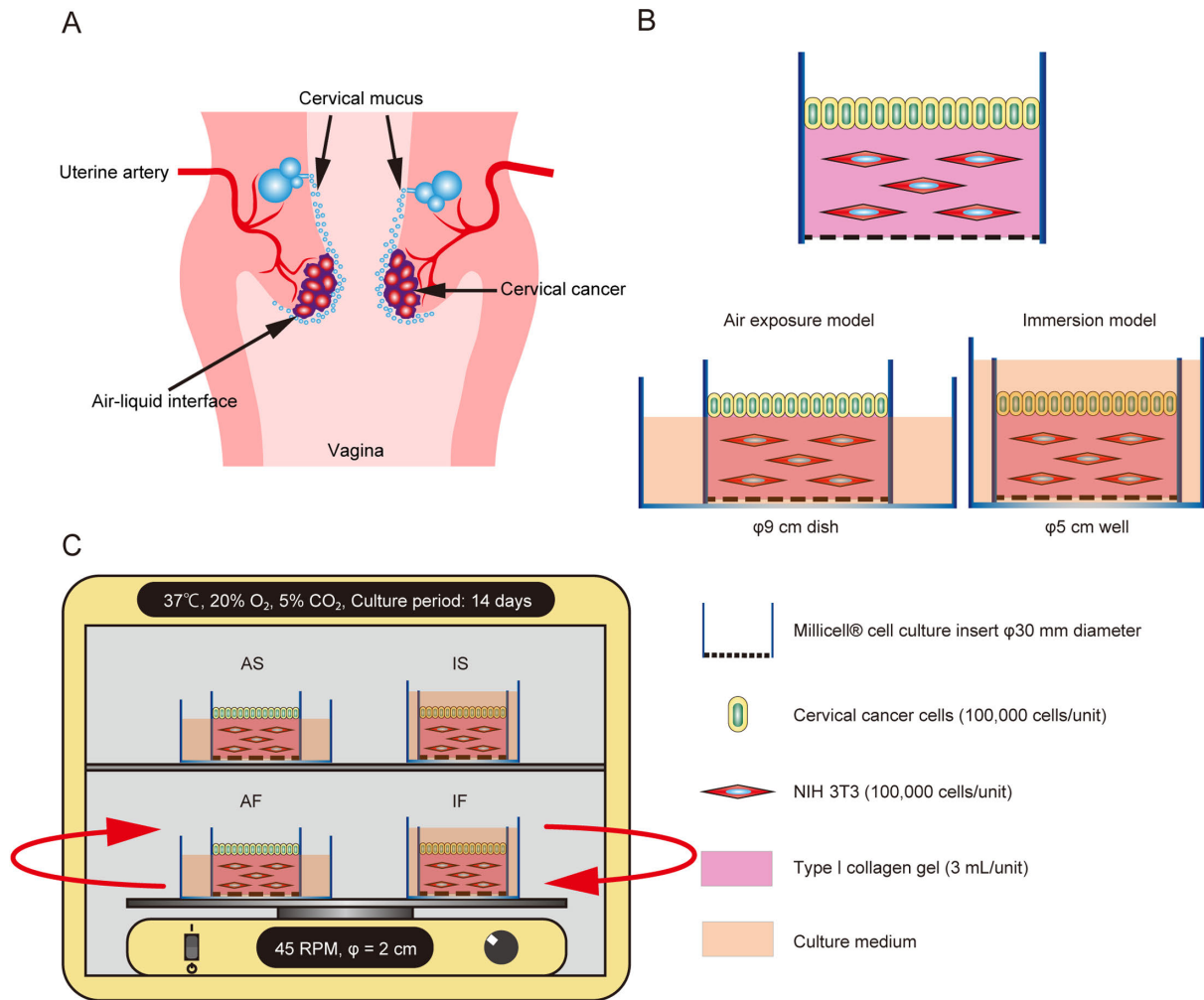
Fig. 1. Schematic illustration of the specific microenvironments of cervical cancer and the culture model. (**A**) Schematic illustration of the specific microenvironments of cervical cancer. (**B**) Illustrations showing the collagen gel culture model and the double-dish air-liquid interface culture method. To replicate the air-liquid interface, the culture fluid level of the outer dish was adjusted to be at the height of the collagen gel in the inner dish. Cervical cancer cells were seeded on a collagen gel embedded with NIH 3T3 cells or a collagen gel without NIH 3T3 cells (control). (**C**) To generate fluid flow, culture dishes were placed on a rotatory shaker in a CO_2 incubator. The cells were cultured under 4 conditions, namely immersion under static flow (IS), immersion under dynamic flow (IF), air exposure under static flow (AS) and air exposure under dynamic flow (AF).

the surroundings cooperate to form a cancer-specific micro-environment. The major cellular components of cervical cancer are squamous cell carcinoma and stromal fibroblasts [16]. Both SCC and stromal fibroblasts are involved in a paracrine loop that regulates the homeostasis and aggressiveness of cervical cancer [24]. Cervical cancer cells are constantly stimulated by the flow of cervical mucus (Fig. 1A). Interstitial fluid flow, which originates from the capillary network, is also normally present in the uterine cervix. In addition, cervical SCC cells at the surface of the uterine cervix are exposed to an air-liquid interface composed of cervical mucus and air. Various research groups, including ours, have reported that fluid flow stimulation is a critical microenvironmental factor for various cells, including cancer cells [1, 14, 17]. Therefore, we speculated that SCC-stromal cell interactions, fluid flow stimulation and the air-liquid interface may play important, and possibly

synergistic, roles in the homeostasis and aggressiveness of cervical cancer cells.

To date, no culture models have been developed that can simultaneously reconstruct tumor-stroma interactions and fluid streaming at an air-liquid interface. Furthermore, little is known about variations in the influence of the microenvironment due to differences in the infecting HPV type.

In the present study, we have overcome this challenge by establishing a simple culture model that can concurrently replicate the biological and physical microenvironments of cervical cancer. The aims were to clarify the impact of biological and physical microenvironmental factors on the homeostasis and aggressiveness of cervical cancer cells.

II. Materials and Methods

Cells

Three cervical SCC cell lines were used in the study namely HPV16-positive Ca Ski (Japanese Cancer Research Bank [JCRB], Osaka, Japan), HPV18-positive HCS-2 (JCRB) and HPV68-positive ME-180 (JCRB). Mouse fibroblast NIH 3T3 cells (JCRB) were also utilized. All cell lines were cultured in RPMI 1640 medium supplemented with 10% fetal bovine serum, 100 μg/mL streptomycin and 100 μg/mL penicillin, and the cells were incubated in a humidified atmosphere containing 5% CO_2 and 20% O_2 at 37°C.

Culture model

We developed a double-dish culture system (Fig. 1B) to analyze the influences of cell-cell interactions and the air-liquid interface on cervical cancer cells [26]. First, NIH 3T3 cells were mixed with a collagen gel solution (Cellmatrix, type I–A; Nitta Gelatin Co., Ltd., Osaka, Japan). Then, 3 mL of the mixture (including 5×10^5 keratocytes or NIH 3T3 cells) was added to 30-mm-diameter Millicell-CM dishes (Millipore, Bedford, MA, USA). After solidification of the gel at 37°C for 30 min, 1×10^5 cervical cancer cells were seeded onto the surface of each dish. To replicate air exposure, these inner dishes were then placed in larger (90-mm-diameter) outer dishes (Sumitomo Bakelite, Co., Ltd., Tokyo, Japan) containing 10 mL of culture medium. Cervical cancer cells were also seeded in collagen gel dishes without mesenchymal cells to serve as controls. For immersion culture, the inner dish was placed in 5-cm-diameter 6-well plates containing 10 mL of culture medium.

Fluid flow-generating system

The fluid flow-generating system was slightly modified from our previously published method [2]. One day after the seeding of cervical cancer cells, culture dishes were incubated in an atmosphere containing 5% CO_2 and 20% O_2 at 37°C. Fluid flow was generated by placing the dishes on a gyratory shaker (Shake-LR; TAITEC, Saitama, Japan) that rotated at a speed of 45 revolutions per min. Static flow conditions were achieved by placing the dishes in a conventional CO_2 incubator. In this way, the cervical cancer cells were exposed to both an air-liquid interface and dynamic flow, thereby mimicking, as closely as possible experimentally, the *in vivo* physical microenvironment of the uterine cervix.

Experimental groups

Cervical cancer cells in monoculture or co-cultured with fibroblast cells were exposed to 4 different physical conditions: immersion culture under static flow conditions (IS); air exposure under static flow conditions (AS); immersion culture under dynamic flow conditions (IF); and air exposure under dynamic flow conditions (AF) (Fig. 1C).

Histology, immunohistochemistry and morphometric analyses

After 14 days of culture, cells were fixed with 10% formalin, routinely processed and embedded in paraffin. Deparaffinized sections were generated and histological observations were made after standard hematoxylin-eosin (HE) staining. Silver impregnation was used to evaluate the depth of cancer cell invasion. Proliferative cells were labeled with a mouse monoclonal anti-Ki-67 antibody (#M7240, Dako, Agilent Technologies, Santa Clara, CA, USA). Apoptosis of cells was detected using anti-cleaved caspase-3 antibodies (#9664; Cell Signaling Technology (CST), Danvers, MA, USA). Immunostaining for Ki-67 and cleaved caspase 3 was detected using Histofine® Simple Stain MAX PO (Nichirei, Tokyo, Japan). The percentages of Ki-67-positive cells and cleaved caspase-3-positive cells were determined as indicators of proliferation and apoptosis, respectively. The cancer cell layer thickness was measured in 10 areas in each of 5 randomly selected non-contiguous and non-overlapping areas (low magnification, ×10 objective). The depth of cancer cell invasion was measured from the basement membrane to the deepest region of the cancer cells.

Western blot analysis

To prepare cells for protein extraction, the cancer cells were co-cultured using plastic inserts with 8-μm pores (Falcon Cell Culture Insert; Becton Dickinson, Franklin, NJ, USA). 5.0×10^5 NIH 3T3 cells embedded in 1 mL of collagen gel were placed on the outer lower part of the plastic insert, and 5.0×10^5 cancer cells were seeded inside the insert. The inserts were then placed in 10-cm-diameter dishes containing 40 mL of complete medium. After 48 hr of culture, the collagen gel was stripped from the plastic inserts. The cancer cells were lysed in 400 μL of M-PER Reagent (Thermo Fisher Scientific, Waltham, MA, USA) supplemented with a protease-phosphatase inhibitor cocktail (CST). Lysates containing an equal quantity of protein were separated by sodium dodecyl sulfate-polyacrylamide gel electrophoresis in 12% Bis-Tris gels and transferred to polyvinylidene fluoride membranes. The membranes were incubated overnight at 4°C with antibodies against extracellular signal-regulated kinase (ERK) 1/2 (#9102; CST), p-ERK1/2 (#4370; CST), p38 (#8690; CST) and p-p38 (#4511; CST). Antibody-bound antigens on the membranes were visualized using a chemiluminescence immunodetection system (Western Breeze; Thermo Fisher Scientific). Band densities were determined and analyzed using a FUSION system (Vilber-Lourmat, Eberhardzell, Germany) and analyzed with ImageJ software (National Institutes of Health [NIH], Bethesda, MD, USA).

Statistical analysis

Data from 3–5 independent experiments were analyzed using Student's t-test or Wilcoxon's test depending on the equality of variance. We used the mean values

of replicates in experiments to determine statistical significance and a *P*-value < 0.05 was taken to indicate a statistically significant finding. All statistical analyses were performed using JMP Pro 14 for Windows (SAS, Cary, NC, USA).

III.   Results

The physical and biological microenvironments synergistically affect cervical cancer cell behavior

To investigate whether the biological and physical microenvironments exerted synergistic effects on cervical SCC, cervical cancer cells in monoculture or co-cultured with fibroblasts were exposed to different biological and physical conditions (Fig. 1C) namely immersion culture under static flow (IS), immersion culture under dynamic flow (IF), air exposure under static flow (AS) or air exposure under dynamic flow (AF). As shown in Fig. 2A, Ca Ski, ME-180 and HCS-2 cells cultured without NIH 3T3 cells under IS conditions had a flat cytoplasm, exhibited a one-to-two layer structure and invaded the collagen matrix at only a few locations. Under IF conditions, monocultured Ca Ski and ME-180 cells exhibited cytoplasmic hypertrophy, and monocultured Ca Ski, HCS-2 and ME-180 cells exhibited significant thickening of the cellular layer when compared with cells maintained under IS conditions. Monocultured Ca Ski, HCS-2 and ME-180 cells under AS conditions had a significantly thicker cellular layer than cells monocultured under IS or IF conditions. In cells exposed to air, dynamic flow promoted the thickness of the cellular layer for ME-180 and HCS-2 cells but not Ca Ski cells. In the absence of mesenchymal cells, dynamic flow and air exposure did not affect the invasive growth of any of the 3 cervical cancer cell types. The cellular layer thicknesses of the various groups shown in Table 1 and Fig. 2B.

Next, we replicated the cancer cell-mesenchymal cell interactions to evaluate whether the biological and physical microenvironments had synergistic effects on the cervical cancer cells. Co-culture with NIH 3T3 cells increased the cellular layer thickness of Ca Ski and HCS-2 cells but not ME-180 cells under IS conditions. Ca Ski cells co-cultured with NIH 3T3 cells under AS conditions exhibited a reduced cellular layer thickness when compared to monocultured Ca Ski cells under AS conditions. Dynamic flow and air exposure increased the cellular layer thicknesses of Ca Ski, HCS-2 and ME-180 cells co-cultured with NIH 3T3 cells. Air exposure increased the cellular layer thickness of all 3 cervical cancer cell types under static flow conditions. Under air exposure conditions, dynamic flow further promoted the cellular layer thickness of Ca Ski, ME-180 and HCS-2 cells co-cultured with NIH 3T3 cells.

The physical and biological microenvironments synergistically affect the growth and survival of cervical cancer cells

We evaluated the proliferative activity and apoptosis of cancer cells using the proliferating cell marker, Ki-67, and the apoptotic cell marker, cleaved caspase-3 (Fig. 3). Under monoculture conditions, exposure to dynamic flow or exposure to air significantly increased the number of Ki-67-positive HCS-2 and ME-180 cells compared to cells exposed to IS conditions. Furthermore, dynamic flow and air exposure synergistically increased the number of Ki-67-positive HCS-2 and MH-180 cells. Dynamic flow and air exposure did not affect the growth of Ca Ski cells.

Co-culture with NIH 3T3 cells increased the number of Ki-67-positive HCS-2 cells under IS, AS and AF conditions and the number of Ki-67-positive ME-180 cells under IS conditions but decreased the number of Ki-67-positive ME-180 cells under IF, AS and AF conditions. Co-culture with NIH 3T3 cells did not affect the growth of Ca Ski cells. Under co-culture and dynamic flow conditions, air exposure synergistically increased the number of Ki-67-positive HCS-2 cells. The number of Ki-67-positive HCS-2 cells observed was less under IF or AS conditions than under IS conditions.

When compared with monocultured cells maintained under IS conditions, dynamic flow and air exposure significantly decreased the number of cleaved caspase-3-positive Ca Ski and ME-180 cells. Furthermore, air exposure reduced the number of cleaved caspase-3-positive HCS-2 cells monocultured under dynamic flow conditions. The Ki-67 positive rates for the various groups are shown in Table 2.

Co-culture with NIH 3T3 cells decreased the number of cleaved caspase-3-positive Ca Ski cells under IS, IF, AS and AF conditions. In contrast, co-culture with NIH 3T3 cells increased the number of cleaved caspase-3-positive HCS-2 cells under IS, AS and AF conditions. Under co-culture conditions, dynamic flow or air exposure downregulated the number of cleaved caspase-3-positive Ca Ski cells. Dynamic flow and air exposure decreased the number of cleaved caspase-3-positive ME-180 cells co-cultured with NIH 3T3 cells, and the effects of dynamic flow and air exposure were synergistic. The cleaved caspase-3 positive rates for the various groups are shown in Table 3.

Regulation of the invasive ability of cervical cancer cells by the biological microenvironment is synergistically affected by the physical microenvironment

Invasiveness is characteristic of aggressive cancer that is associated with poor outcomes such as shorter survival times [16]. As shown in Fig. 4, dynamic flow, air exposure or their combination did not affect the invasion depth of monocultured Ca Ski, HCS-2 or ME-180 cells. ME-180 cells co-cultured with NIH 3T3 cells showed a significant increase in invasion depth compared to monocultured cells, and air exposure further enhanced the invasiveness of co-
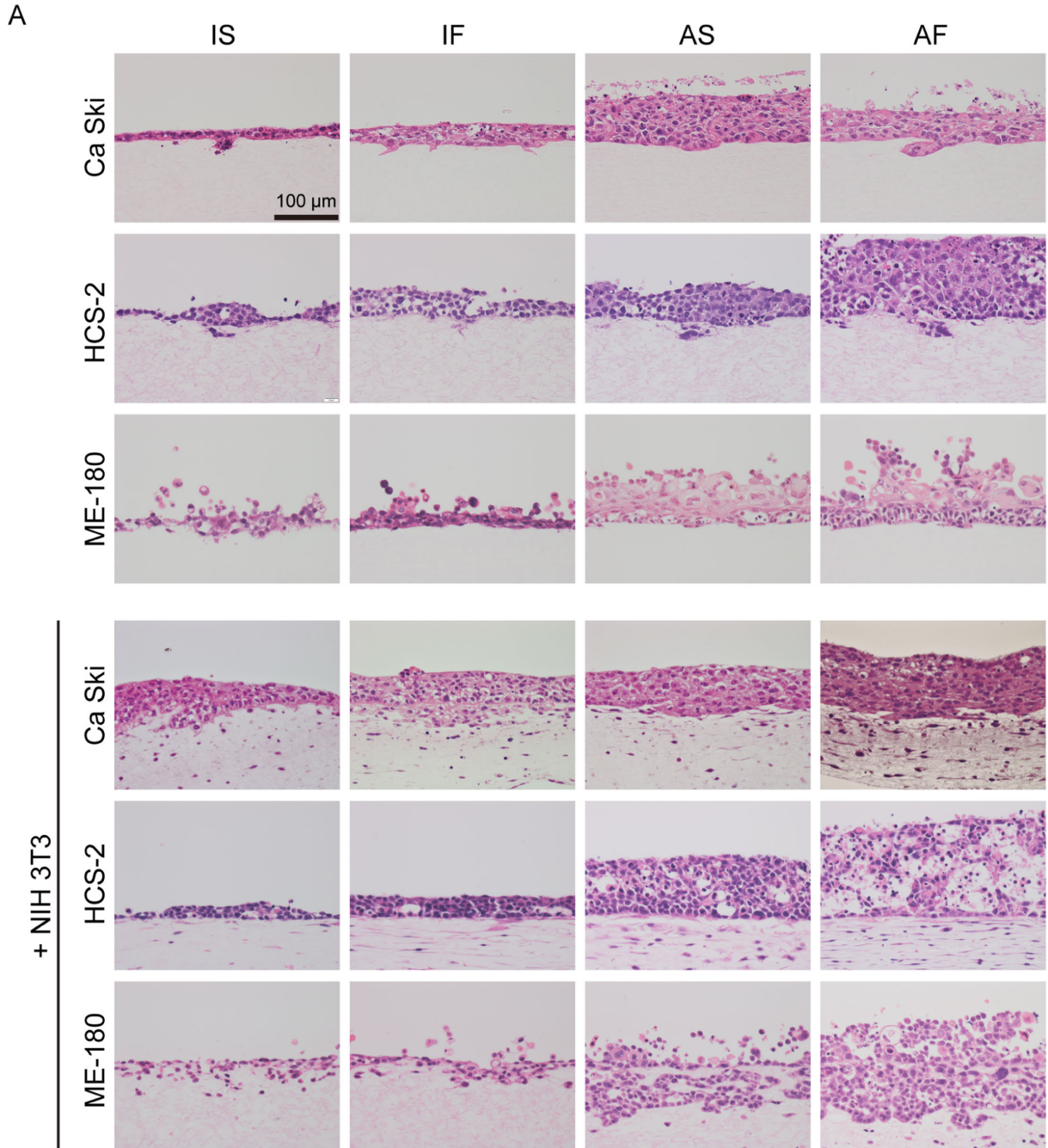
Fig. 2. Effects of fluid flow and air exposure on the cellular kinetics of cervical cancer cells. (**A**) Representative images at day 14. Under IS conditions, Ca Ski, HCS-2 and ME-180 cells cultured without NIH 3T3 cells had a flat cytoplasm, formed a thin layered structure and invaded the collagen matrix at only a few locations. Fluid flow promoted cytoplasmic hypertrophy and thickening of the cellular layer of monocultured Ca Ski, HCS-2 and ME-180 cells. Fluid flow and air exposure synergistically induced cellular hypertrophy and a thickening of the cellular layer of Ca Ski, ME-180 and HCS-2 cells. ME-180 and HCS-2 cells, but not Ca Ski cells, had a thicker cellular layer under AF conditions than under AS conditions. Under IS conditions, NIH 3T3 cells promoted cellular hypertrophy and increased the cellular layer thickness of Ca Ski cells but not the other cell types. Fluid flow increased the cellular layer thickness of HCS-2 cells co-cultured with NIH 3T3 cells, but this effect was not observed in Ca Ski and ME-180 cells. Fluid flow increased the number of invasive spots for Ca Ski cells co-cultured with NIH 3T3 cells. Under static flow conditions, air exposure increased the cellular layer thickness of all 3 cervical cancer cell types. Fluid flow and air exposure significantly increased the cellular layer thickness of Ca Ski and ME-180 cells. By contrast, HCS-2 cells co-cultured with NIH 3T3 cells exhibited less thickening of the cellular layers and a smaller degenerative area under AF conditions. Bar = 100 μm. (**B**) The thickness of the cellular layers. $*P < 0.05$. $**P < 0.001$. Abbreviations: AF, air exposure under dynamic flow; AS, air exposure under static flow; IF, immersion under dynamic flow; IS, immersion under static flow. Data are shown as the mean ± standard deviation of 3 measurements.
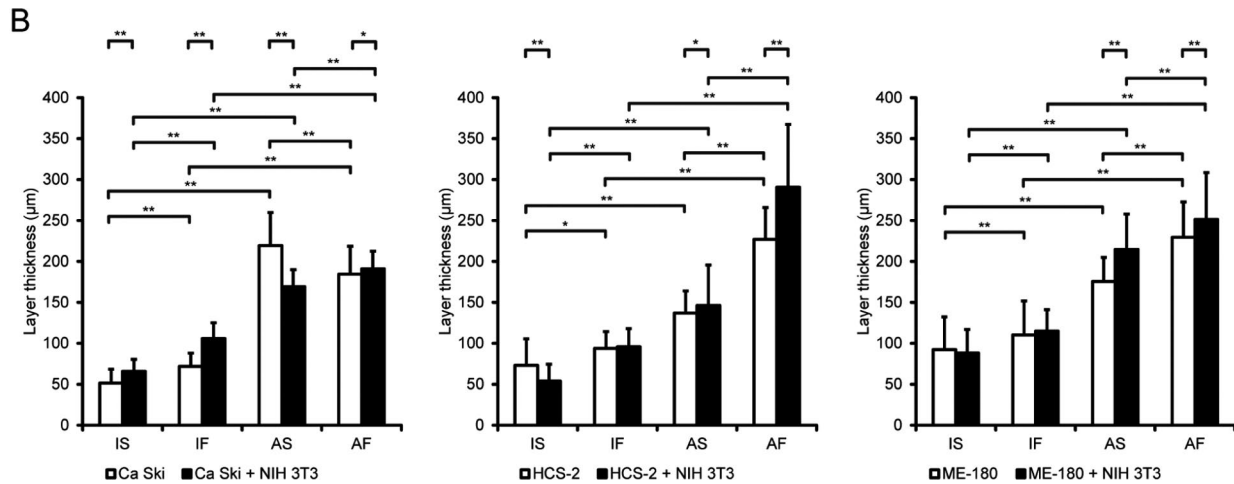
B

Fig. 2. Continued.

Table 1. *Layer thicknesses of cervical cancer cells*

Groups	Conditions	Ca Ski (μm)	HCS-2 (μm)	ME-180 (μm)
Mono				
	IS	54.4 ± 16.9	80.8 ± 32.9	92.1 ± 39.9
	IF	72.1 ± 16.0	93.8 ± 20.4	110.1 ± 41.6
	AS	219.2 ± 40.5	137.0 ± 26.8	175.4 ± 29.3
	AF	184.3 ± 33.9	226.8 ± 38.8	229.3 ± 43.3
+ NIH 3T3				
	IS	65.5 ± 14.8	56.0 ± 20.5	88.0 ± 28.8
	IF	105.7 ± 19.3	95.8 ± 22.1	114.8 ± 26.1
	AS	169.1 ± 20.5	146.2 ± 49.2	214.6 ± 43.1
	AF	190.7 ± 21.6	290.7 ± 76.6	251.3 ± 57.3

cultured ME-180 cells. The invasion depth of Ca Ski cells co-cultured with NIH 3T3 cells was significantly enhanced by dynamic flow stimulation, and air exposure acted synergistically to promote this effect of dynamic flow. In contrast, co-culture with NIH 3T3 cells inhibited the invasive properties of HCS-2 cells under IS, IF, AS and AF conditions. The invasion depths for the various groups are shown in Table 4.

The biological and physical microenvironments synergistically modulated the expression of p38 and ERK1/2 in cervical SCC cells

Mitogen-activated protein kinase (MAPK) pathways have been widely shown to play a role in the aggressiveness, proliferation, epithelial-mesenchymal transition and invasiveness of many cancer cell types [5]. Therefore, we measured the expression of ERK1/2 and p38 in Ca Ski, HCS-2 and ME-180 cells to evaluate whether the biological and physical microenvironments influenced MAPK signaling.

As shown in Fig. 5, total ERK1/2 expression in Ca Ski cells cultured with or without NIH 3T3 cells was not affected by dynamic flow or air exposure. Dynamic flow increased the phosphorylated/total ERK1/2 ratio in monocultured Ca Ski cells under immersion conditions.

Co-culture with NIH 3T3 cells significantly decreased the phosphorylated/total ERK1/2 ratio in Ca Ski cells under IF or AS conditions. When compared to cells maintained under IS conditions, the phosphorylated/total ERK1/2 ratio in Ca Ski cells co-cultured with NIH 3T3 cells was reduced by dynamic flow (IF) or air exposure (AS) but not by a combination of dynamic flow and air exposure (AF). Total p38 expression in monocultured Ca Ski cells was downregulated by air exposure with or without dynamic flow, but no such effects were observed on Ca Ski cells co-cultured with NIH 3T3 cells. Air exposure with or without dynamic flow significantly increased the phosphorylated/total p38 ratio in monocultured Ca Ski cells. Co-culture with NIH 3T3 cells decreased the phosphorylated/total p38 ratio in Ca Ski cells under AS or AF conditions but not under IS or IF conditions.

Total ERK1/2 expression in monocultured HCS-2 cells was significantly upregulated by air exposure with or without dynamic flow. Co-culture with NIH 3T3 cells decreased total ERK1/2 expression in HCS-2 cells under AF conditions. The phosphorylated/total ERK1/2 ratio in monocultured HCS-2 cells was decreased by air exposure under static flow conditions. Co-culture with NIH 3T3 cells decreased the phosphorylated/total ERK1/2 ratio in HCS-2 cells under IS conditions. Dynamic flow, air exposure and co-culture with NIH 3T3 cells did not affect total p38 expression in HCS-2 cells. Air exposure significantly upregulated the phosphorylated/total p38 ratio in monocultured HCS-2 cells under AS and AF conditions. Co-culture with NIH 3T3 cells decreased the phosphorylated/total p38 ratio in HCS-2 cells under AF conditions.

Total ERK1/2 expression in ME-180 cells cultured with or without NIH 3T3 cells was not affected by dynamic flow or air exposure. Dynamic flow and air exposure decreased the phosphorylated/total ERK1/2 ratio in monocultured ME-180 cells. Co-culture with NIH 3T3 cells significantly upregulated the phosphorylated/total ERK1/2 ratio in ME-180 cells under IF, IF and AF conditions.
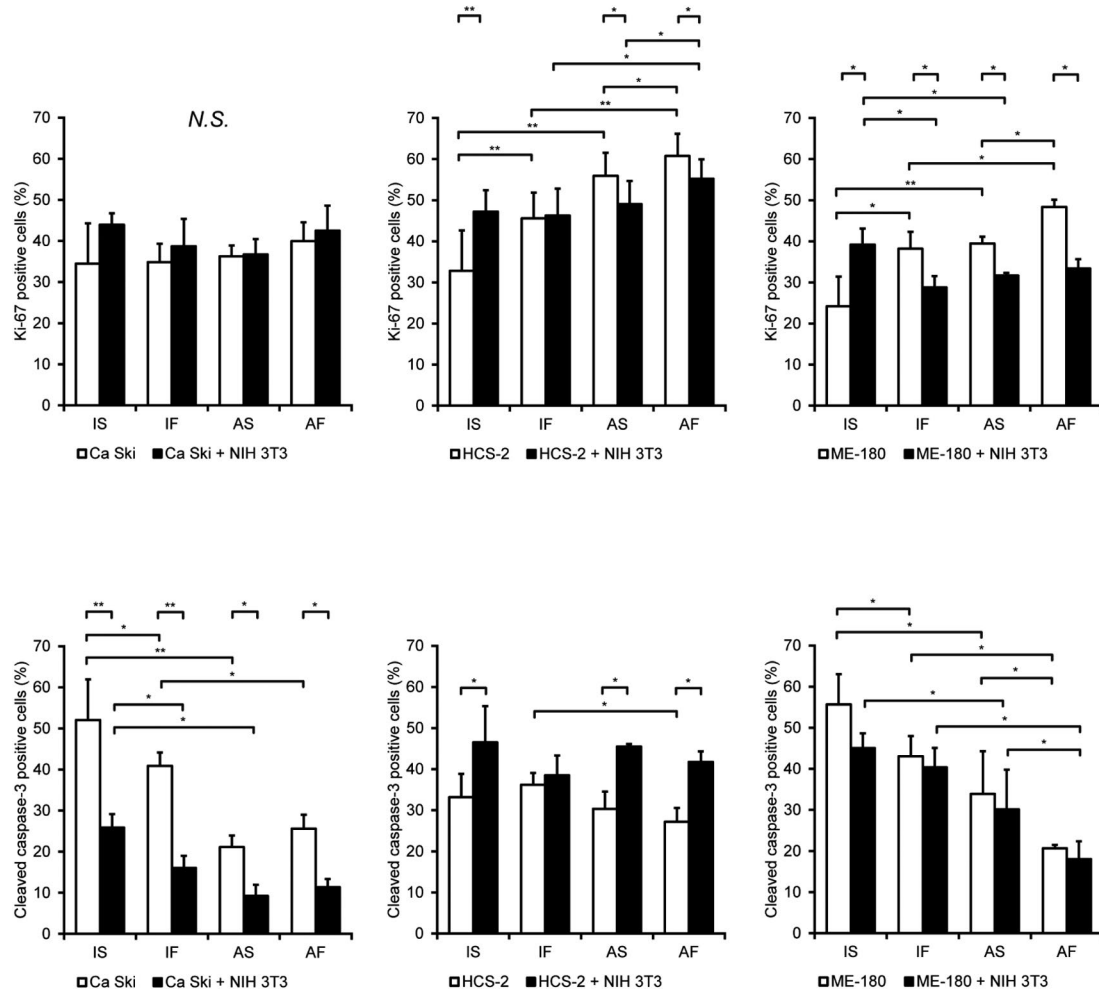
Fig. 3. Effects of fluid flow and air exposure on the proliferative activity and apoptosis of cervical cancer cells. The percentages of cells positively immunostained for Ki-67 and cleaved caspase-3. Data are shown as the mean ± standard deviation of 3 measurements. *$P < 0.05$. **$P < 0.001$.

Table 2. *Ki-67 positive rates of cervical cancer cells*

Groups	Conditions	Ca Ski (%)	HCS-2 (%)	ME-180 (%)
Mono				
	IS	34.5 ± 9.8	32.8 ± 9.9	24.2 ± 7.2
	IF	34.9 ± 4.4	45.6 ± 6.2	38.2 ± 4.1
	AS	36.2 ± 2.7	55.9 ± 5.6	39.4 ± 1.7
	AF	39.9 ± 2.6	60.7 ± 5.4	48.3 ± 1.7
+ NIH 3T3				
	IS	43.9 ± 2.8	47.2 ± 5.2	39.2 ± 3.9
	IF	38.7 ± 6.7	46.2 ± 6.5	28.8 ± 2.8
	AS	36.7 ± 3.8	49.0 ± 5.6	31.6 ± 0.6
	AF	42.5 ± 6.1	55.3 ± 4.7	33.4 ± 2.3

Table 3. *Cleaved caspase-3 positive rates of cervical cancer cells*

Groups	Conditions	Ca Ski (%)	HCS-2 (%)	ME-180 (%)
Mono				
	IS	52.0 ± 9.9	33.2 ± 5.7	55.7 ± 7.3
	IF	40.9 ± 3.2	36.2 ± 2.9	43.1 ± 4.9
	AS	21.1 ± 2.8	30.4 ± 4.2	33.9 ± 10.4
	AF	25.6 ± 3.4	27.2 ± 3.3	2.7 ± 0.9
+ NIH 3T3				
	IS	25.9 ± 3.3	46.5 ± 8.8	45.0 ± 3.6
	IF	16.1 ± 2.9	38.5 ± 4.9	40.3 ± 4.8
	AS	9.2 ± 2.7	45.5 ± .6	30.1 ± 9.7
	AF	11.4 ± 2.0	41.8 ± 2.6	18.0 ± 4.3

The phosphorylated/total ERK1/2 ratio in ME-180 cells co-cultured with NIH 3T3 cells under the AF condition was significantly lower than for the IF condition. Air exposure significantly upregulated the phosphorylated/total ERK1/2 ratio in ME-180 cells without NIH 3T3 cells under static flow and dynamic flow conditions Under IS and IF con-

ditions, NIH 3T3 cells increased total p38 expression in ME-180 cells compared to the monoculture group. Air exposure under dynamic flow significantly increased the phosphorylated/total p38 ratio in ME-180 cells co-cultured with NIH 3T3 cells.
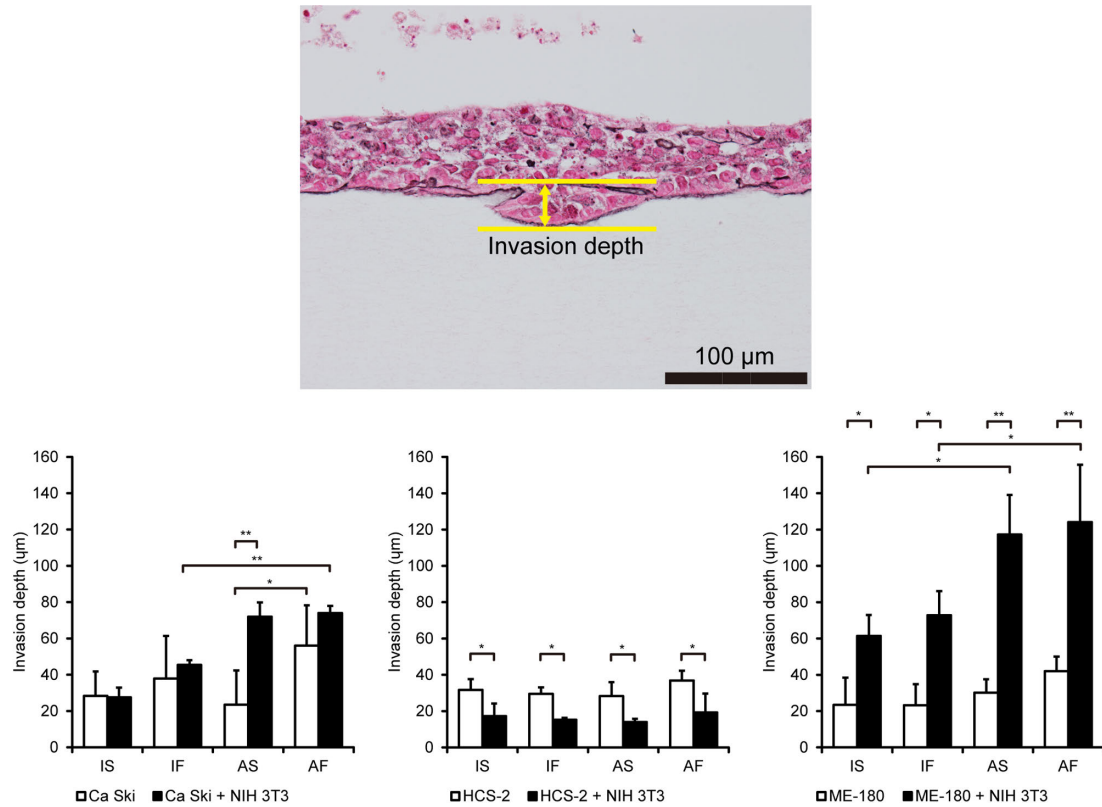
Fig. 4. Fluid flow and air exposure promote the invasiveness of cervical cancer cells. The upper panel shows a representative image illustrating the measurement of invasion depth and the number of invading cells. The lower panels compare invasion depth between the various experimental groups. Data are shown as the mean ± standard deviation of 3 measurements. *$P < 0.05$. **$P < 0.001$. Bar = 100 μm. Abbreviations: AF, air exposure under dynamic flow; AS, air exposure under static flow; IF, immersion under dynamic flow; IS, immersion under static flow.

Table 4. *The invasion depths of cervical cancer cells*

Groups	Conditions	Ca Ski (μm)	HCS-2 (μm)	ME-180 (μm)
Mono				
	IS	28.4 ± 13.3	31.7 ± 6.0	23.4 ± 15.0
	IF	37.9 ± 23.5	29.5 ± 3.6	23.3 ± 11.5
	AS	23.5 ± 18.9	28.3 ± 7.7	30.2 ± 7.4
	AF	56.0 ± 22.3	36.9 ± 5.3	42.0 ± 8.0
+ NIH 3T3				
	IS	27.6 ± 5.3	17.2 ± 6.9	61.4 ± 11.5
	IF	45.5 ± 2.5	15.2 ± 1.1	72.8 ± 13.3
	AS	72.0 ± 7.9	14.0 ± 1.8	117.2 ± 21.8
	AF	74.0 ± 4.0	19.3 ± 10.4	124.1 ± 31.6

IV. Discussion

In the present study, we demonstrated that a biological microenvironmental factor and two physical microenvironmental factors act synergistically to regulate the aggressiveness and survival of cervical cancer cells.

Many studies have reported that cancer-associated fibroblasts modulate the kinetics of various cancer cell types through paracrine effects [23, 28]. In addition, physical microenvironmental factors such as shear stress and fluid flow stimulation have recently been recognized to influence the development of various cell types, including cancer and stem cells [12, 19]. Shear stress and fluid flow stimulation are key regulators of normal and cancer tissue proliferation, but the relationships between biological and physical microenvironmental factors have not yet been fully elucidated. One reason for this is that three-dimensional models replicating both the biological and physical microenvironments had not been previously established. Recently, it has been suggested that fluid flow stimulation and cell-cell interactions mutually regulate cell kinetics and drug sensitivity [1, 6]. Our rather simple culture model enabled accurate evaluation of the proliferation and apoptosis of cervical cancer cells and revealed cancer cell invasion into the stroma similar to that observed *in vivo*.

Epidemiological studies have revealed that HPV infection is the main cause of invasive squamous cell carcinoma and its precursor lesions [27]. Clifford *et al.* reported that high-grade squamous intraepithelial lesions (HSILs) infected with HPV16, HPV18 or HPV45 preferentially progress to SCC when compared to HSILs infected with HPV31, HPV33, HPV52 or HPV58 [7]. Changes in the
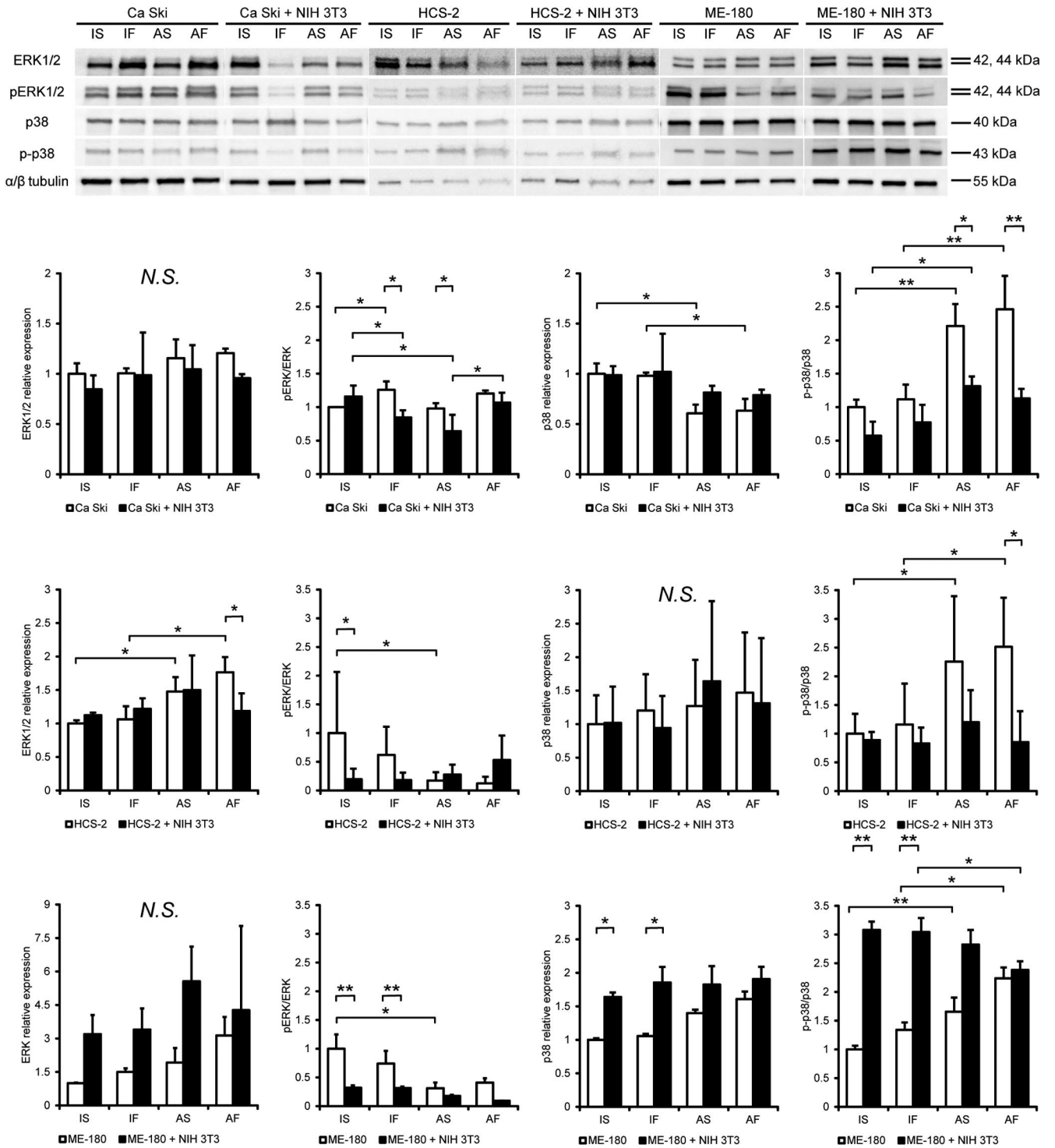
Fig. 5. Effects of fluid flow, air exposure and NIH 3T3 cells on MAPK expression in cervical cancer cells. Protein expression levels in cervical cancer cells evaluated by western blotting. Target protein expression was determined relative to that of α/β tubulin expression. The expression of each protein was normalized to the mean expression level in monocultured cells under IS conditions. Data are presented as the mean ± standard deviation of 3–5 determinations. *$P < 0.05$. **$P < 0.001$. Abbreviation: AF, air exposure under dynamic flow; AS, air exposure under static flow; IF, immersion under dynamic flow; IS, immersion under static flow; MAPK, mitogen-activated protein kinase.

expression of oncoproteins such as E5, E6 and E7 in HPV infected cells, due to various microenvironments including the state after carcinogenesis and cancer development, have not been elucidated. Furthermore, the kinetics of cells infected with different HPV types have not yet been determined after malignant transformation. We found that the biological and physical microenvironments synergistically regulated the proliferative activity and apoptosis of all 3 cervical cancer cell lines in a similar fashion. Notably, NIH 3T3 cells promoted the invasiveness of Ca Ski and ME-180 cells but suppressed the invasiveness of HCS-2 cells. Stromal cells are known to increase the invasiveness of cancer cells [13, 29], and the findings of the present study indicate that the effects of microenvironmental factors differ depending on the cancer cell type. It was beyond the scope of the present study to clarify the precise mechanisms underlying the above phenomena relevant to different microenvironments, so further research is needed.

The crucial limitation in the present study was that we could not elucidate the precise mechanism of behavioral changes exhibited by each cancer cell type.

Activation of MAPK signaling is widely recognized as a key factor in the survival, proliferation, dissemination and metabolism of human cancers [5], and high-risk HPV protein E5 seems to play a role in the activation of MAPK signaling [8]. Ca Ski, HCS-2 and ME-180 cells were infected with high-risk HPVs, and we predicted that the MAPK pathway induces similar expression changes to these 3 cancer types depending on the microenvironments. Contrary to expectations, the result demonstrated that dynamic flow, air exposure and cell-cell interactions could regulate the activation of the MAPK pathway, but reactivity against microenvironment types were different for each cancer cell and did not show a specific tendency. ERK1 is a fundamental molecule in MAPK signaling and has been shown to control proliferation, apoptosis and differentiation of cells in cervical cancer that is associated with HPV infection [4, 15]. We suspect that there is no commonality in the expression of this basic protein, and it should be considered that control by the microenvironment differs greatly according to the cell type, including the type of HPV. HPV integration sites have been reported to be MYC, ERBB2, GLI2, TNIK, NR4A2, PROX1, EIF2C2, FAM179B, and SERPINB4, RPS6KB1, MAFA, PARN, EGFL7, SNIP1, POC1B, and BCL11B [20, 22]. We should also consider major cellular regulatory pathways such as PIK3CA, PTEN, TP53, STK11 and KRAS to understand the dynamic regulation of cervical cancer cells [10, 11, 18].

In conclusion, we have established an experimental model system that can be used to investigate concurrently the effects of the biological and physical microenvironment on cervical cancer. This new model system could be a promising research tool to facilitate investigations into treatments for cervical cancer.

V. Conflicts of Interest

The authors declare that they have no conflicts of interest.

VI. Acknowledgments

VII. References

1. Akutagawa, T., Aoki, S., Yamamoto-Rikitake, M., Iwakiri, R., Fujimoto, K. and Toda, S. (2018) Cancer–adipose tissue interaction and fluid flow synergistically modulate cell kinetics, HER2 expression, and trastuzumab efficacy in gastric cancer. *Gastric Cancer* 21; 946–955.
2. Aoki, S., Makino, J., Nagashima, A., Takezawa, T., Nomoto, N., Uchihashi, K., *et al.* (2011) Fluid flow stress affects peritoneal cell kinetics: possible pathogenesis of peritoneal fibrosis. *Perit. Dial. Int.* 31; 466–476.
3. Arbyn, M., Weiderpass, E., Bruni, L., de Sanjosé, S., Saraiya, M., Ferlay, J., *et al.* (2020) Estimates of incidence and mortality of cervical cancer in 2018: a worldwide analysis. *Lancet Glob. Health* 8; e191–e203.
4. Bai, L., Mao, R., Wang, J., Ding, L., Jiang, S., Gao, C., *et al.* (2015) ERK1/2 promoted proliferation and inhibited apoptosis of human cervical cancer cells and regulated the expression of c-Fos and c-Jun proteins. *Med. Oncol.* 32; 57.
5. Burotto, M., Chiou, V. L., Lee, J. M. and Kohn, E. C. (2014) The MAPK pathway across different malignancies: a new perspective. *Cancer* 120; 3446–3456.
6. Chen, M. B., Srigunapalan, S., Wheeler, A. R. and Simmons, C. A. (2013) A 3D microfluidic platform incorporating methacrylated gelatin hydrogels to study physiological cardiovascular cell–cell interactions. *Lab Chip* 13; 2591–2598.
7. Clifford, G., Smith, J., Aguado, T. and Franceschi, S. (2003) Comparison of HPV type distribution in high-grade cervical lesions and cervical cancer: a meta-analysis. *Br. J. Cancer* 89; 101–105.
8. Crusius, K., Rodriguez, I. and Alonso, A. (2000) The Human Papillomavirus Type 16 E5 Protein Modulates ERK12 and p38 MAP kinase Activetion by an EGFR-Independent Process in Stressed Human Keratinocytes. *Virus Genes* 20; 65–69.
9. Feig, C., Gopinathan, A., Neesse, A., Chan, D. S., Cook, N. and Tuveson, D. A. (2012) The pancreas cancer microenvironment. *Clin. Cancer Res.* 18; 4266–4276.
10. Hirose, S., Murakami, N., Takahashi, K., Kuno, I., Takayanagi, D., Asami, Y., *et al.* (2020) Genomic alterations in STK11 can predict clinical outcomes in cervical cancer patients. *Gynecol. Oncol.* 156; 203–210.
11. Hu, Z. and Ma, D. (2018) The precision prevention and therapy of HPV-related cervical cancer: new concepts and clinical implications. *Cancer Med.* 7; 5217–5236.
12. Hyler, A. R., Baudoin, N. C., Brown, M. S., Stremler, M. A., Cimini, D., Davalos, R. V., *et al.* (2018) Fluid shear stress impacts ovarian cancer cell viability, subcellular organization,

and promotes genomic instability. *PLoS One* 13; e0194170.

13. Kalluri, R. and Zeisberg, M. (2006) Fibroblasts in cancer. *Nat. Rev. Cancer* 6; 392–401.

14. Kawata, K., Aoki, S., Futamata, M., Yamamoto-Rikitake, M., Nakao, I., Enaida, H., *et al.* (2019) Mesenchymal cells and fluid flow stimulation synergistically regulate the kinetics of corneal epithelial cells at the air–liquid interface. *Graefes Arch. Clin. Exp. Ophthalmol.* 257; 1915–1924.

15. Kim, S.-H., Juhnn, Y.-S., Kang, S., Park, S.-W., Sung, M.-W., Bang, Y.-J., *et al.* (2006) Human papillomavirus 16 E5 up-regulates the expression of vascular endothelial growth factor through the activation of epidermal growth factor receptor, MEK/ERK1, 2 and PI3K/Akt. *Cell. Mol. Life Sci.* 63; 930–938.

16. Kumar, V., Abbas, A. K., Fausto, N. and Aster, J. C. (2014) Robbins and Cotran Pathologic Basis of Disease, Professional Edition e-book, Elsevier Health Sciences.

17. Lee, H. J., Diaz, M. F., Price, K. M., Ozuna, J. A., Zhang, S., Sevick-Muraca, E. M., *et al.* (2017) Fluid shear stress activates YAP1 to promote cancer cell motility. *Nat. Commun.* 8; 1–14.

18. Liu, J., Huang, B., Xiu, Z., Zhou, Z., Liu, J., Li, X., *et al.* (2018) PI3K/Akt/HIF-1α signaling pathway mediates HPV-16 oncoprotein-induced expression of EMT-related transcription factors in non-small cell lung cancer cells. *J. Cancer* 9; 3456.

19. Mitchell, M. J. and King, M. R. (2013) Fluid shear stress sensitizes cancer cells to receptor-mediated apoptosis via trimeric death receptors. *New J. Phys.* 15; 015008.

20. Nair, S. and Pillai, M. (2005) Human papillomavirus and disease mechanisms: relevance to oral and cervical cancers. *Oral Dis.* 11; 350–359.

21. Neesse, A., Algül, H., Tuveson, D. A. and Gress, T. M. (2015) Stromal biology and therapy in pancreatic cancer: a changing paradigm. *Gut* 64; 1476–1484.

22. Ojesina, A. I., Lichtenstein, L., Freeman, S. S., Pedamallu, C. S., Imaz-Rosshandler, I., Pugh, T. J., *et al.* (2014) Landscape of genomic alterations in cervical carcinomas. *Nature* 506; 371–375.

23. Östman, A. and Augsten, M. (2009) Cancer-associated fibroblasts and tumor growth–bystanders turning into key players. *Curr. Opin. Genet. Dev.* 19; 67–73.

24. Pietras, K., Pahler, J., Bergers, G. and Hanahan, D. (2008) Functions of paracrine PDGF signaling in the proangiogenic tumor stroma revealed by pharmacological targeting. *PLoS Med.* 5; e19.

25. Schiffman, M., Castle, P. E., Jeronimo, J., Rodriguez, A. C. and Wacholder, S. (2007) Human papillomavirus and cervical cancer. *Lancet* 370; 890–907.

26. Sugihara, H., Toda, S., Yonemitsu, N. and Watanabe, K. (2001) Effects of fat cells on keratinocytes and fibroblasts in a reconstructed rat skin model using collagen gel matrix culture. *Br. J. Dermatol.* 144; 244–253.

27. Walboomers, J. M., Jacobs, M. V., Manos, M. M., Bosch, F. X., Kummer, J. A., Shah, K. V., *et al.* (1999) Human papillomavirus is a necessary cause of invasive cervical cancer worldwide. *J. Pathol.* 189; 12–19.

28. Xing, F., Saidou, J. and Watabe, K. (2010) Cancer associated fibroblasts (CAFs) in tumor microenvironment. *Front. Biosci.* 15; 166–179.

29. Zhang, Y., Tang, H., Cai, J., Zhang, T., Guo, J., Feng, D., *et al.* (2011) Ovarian cancer-associated fibroblasts contribute to epithelial ovarian carcinoma metastasis by promoting angiogenesis, lymphangiogenesis and tumor cell invasion. *Cancer Lett.* 303; 47–55.